Characterization of Laser-Driven Shock Waves Using Interferometry

K. S. Budil
P. Celliers
G. W. Collins
L. B. Da Silva
R. Cauble
R. J. Wallace
G. Chiu[*]
A. Ng[*]

Introduction

The behavior of materials at high pressures and densities is of great practical interest in a wide variety of fields, from astrophysics to inertial confinement fusion and other related fields where such conditions are routinely encountered. Compression of matter to such extreme conditions requires strong, multi-megabar shock waves for which only a limited number of drivers exist, including nuclear weapons.[1–5] In a laboratory setting, high-power lasers offer great promise for generating the requisite pressures and densities, although the transient nature of the shock wave greatly complicates such experiments.

Researchers first generated multi-megabar, laser-driven shock waves in the 1970s,[6–8] and this early work has been followed by numerous experiments using both direct[9–11] and indirect[12–14] laser drives. These experiments are often criticized because of the nature of laser-driven shock waves: typically, the duration of the laser pulse is quite short (several nanoseconds), so that the steadiness of the shock wave in time is questionable. The starting conditions of the experiment could be changed if the material being targeted were preheated by the x rays or hot electrons from the high-temperature, laser-deposition region well in advance of the arrival of the shock wave. The spatial structure of the shock may not be accurately diagnosed, and there is the possibility that the shock front may either be severely curved or carry small-scale spatial modulations imparted by the laser driver. Thus, accurate characterization of the spatial and temporal characteristics of the shock wave generated by a laser driver is critically important for calculating high-precision equations of state (EOSs) for the target materials.[15]

* University of British Columbia, Vancouver, B. C., Canada.

EOS of Cryogenic D_2

When our project was begun to make a high-precision EOS measurement for cryogenic D_2 in the 1- to 3-Mbar regime, accurate characterization of the laser-driven shock wave was required to ensure that errors were small enough to differentiate between the two proposed EOS models. Because those measurements relied on solving the Hugoniot equations using the initial state of the material prior to arrival of the shock, any change in this state, particularly due to preheat, would have a large impact on the result. Thus, it becomes important to accurately characterize the shock and initial state of the D_2. The results of these measurements are described in the article "Absolute Equation of State Measurements of Compressed Liquid Deuterium Using Nova" on p. 16 of this *Quarterly* and in the literature.[16]

We compressed liquid D_2 with a shock wave generated using one beam of the Nova laser (Figure 1). The laser drive directly irradiates a polystyrene-coated Al flat, ablatively launching a shock wave into the Al "pusher." The shock breaks out the rear surface of this Al pusher and begins to compress the liquid D_2. We used temporally resolved, side-on radiography to diagnose the position of the Al–D_2 interface and the position of the shock front in the D_2. This yielded direct measurements of shock and particle velocities and compression. To accurately characterize the experimental system, we employed a diagnostic technique using interferometry to probe both the initial state of the liquid D_2 (the level of preheating) and the structure of the shock driving the experiment (the shock planarity). The interferometric probe beam was incident through a sapphire window placed at the end of the reservoir containing the liquid D_2, and the rear surface of the Al pusher was diagnosed.

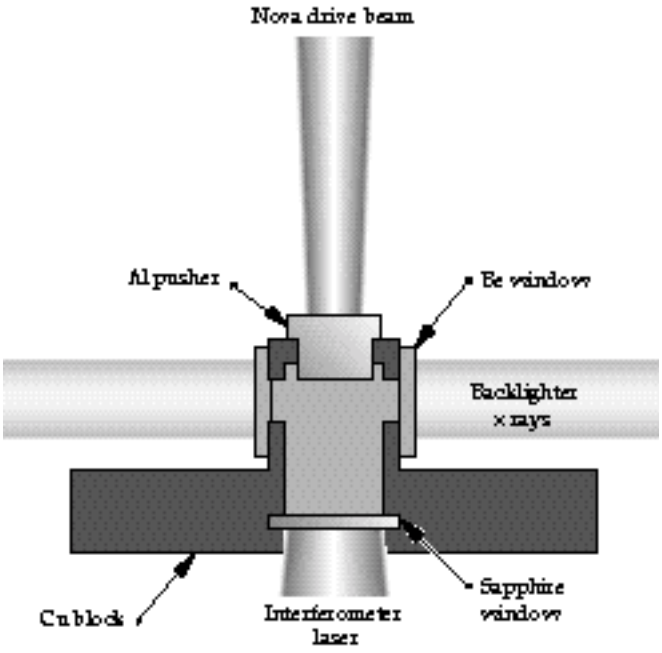

FIGURE 1. Schematic of the cryogenic cell target. One Nova beam is used to ablatively launch a shock wave into a polystyrene-coated Al flat. The shock breaks out the rear surface of this Al pusher and begins to compress the liquid D_2. A laser used as an interferometric probe beam is incident through a sapphire window placed at the end of the reservoir containing the liquid D_2. (08-00-0197-0007pb02)

Interferometric Characterization

Interferometry provides many advantages for characterizing a laser-produced shock wave. Interferometers can be designed with very good spatial resolution and very high temporal sensitivity, allowing extremely accurate measurements of the characteristics of the shock wave. Also, interferometers that measure displacement (the Michelson system)[17] or velocity (Velocity Interferometer System for Any Reflector, VISAR)[18] can be devised to allow investigation of both spatial (shock planarity and preheating) and temporal (shock steadiness) properties. We concentrated on displacement interferometry for our experiments.

Displacement Interferometry

When an unperturbed pulse of light traveling a fixed distance (the reference arm) and a pulse that is reflected from a target surface (the probe arm) are allowed to coherently interfere, the fringe pattern produced provides a measure of the phase difference between the two light paths. If this phase difference changes (for instance, the length of the probe arm begins to increase or decrease because of target motion), a fringe shift will be observed. Therefore, by temporally resolving the output signal from the interferometer with a streak camera, a one-dimensional image of the position of the surface being probed as a function of time is produced. For example, if the pusher is heated in advance of the arrival of the shock wave, the rear surface of the sample will thermally expand, and the initially static fringe pattern will shift. The velocity and extent to which this surface moves can then be correlated to the temperature of the material by comparing our results with numerical simulations of the thermal expansion process.

This same diagnostic also provides a very sensitive probe of the planarity of the shock wave when it breaks through the rear surface of the material. The passage of the strong shock wave results in the formation of a plasma at the rear surface of the target. This causes a dramatic drop in the reflectivity of this surface to the probe beam, which results in a very rapid (50–100 ps) loss of fringe visibility upon shock breakout. The relative timing of the shock breakout across the face of the target then gives a measure of the planarity of the shock wave at this instant in time. Additionally, any spatial modulations imparted to the shock wave by the laser driver will be seen as variations in the shock breakout time across the target.

Experimental Configuration

To determine the level of preheat at the rear surface of the Al pusher and the planarity of the shock wave, we designed an interferometer to probe the target while radiographic measurements were taken. Figure 2 shows a schematic of the Michelson interferometer used in these experiments.

We used a Q-switched Nd:YAG laser operating at the third harmonic (355 nm) with a pulse duration (full

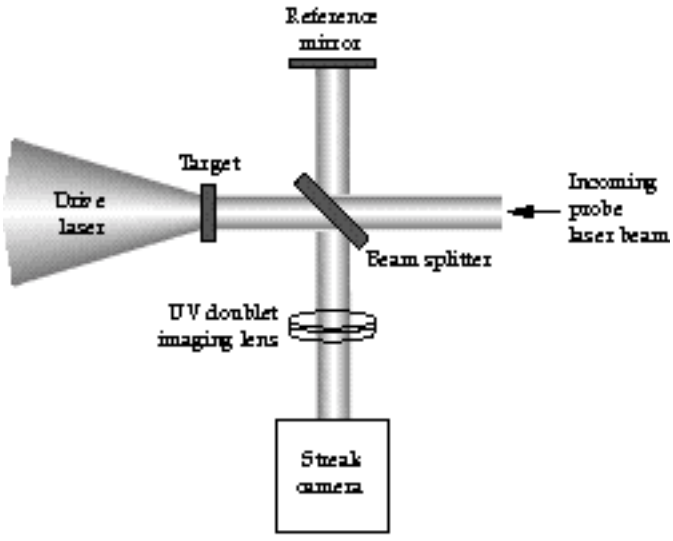

FIGURE 2. Schematic of the Michelson interferometer system showing the reference and target probe arms. The recombined beams are imaged by a UV-doublet lens, and the resulting interference pattern is temporally resolved using a streak camera. (08-00-0197-0013pb01)

width at half maximum) of ~15 ns and ≤1 mJ pulse energy as the probe beam. An f/5 imaging objective (an UV doublet lens combination) was placed external to the interferometer components and imaged the target surface and reference surface simultaneously. The signal generated by the two interfering beams was relayed onto a UV streak camera to provide both spatial and temporal information.

Very small changes in the position of the surface being probed can be detected because a 90° phase shift between the two arms of the interferometer corresponds to a spatial displacement at the target of only $0.5\lambda = 177.3$ nm, and a small fraction of one fringe shift (0.2 fringe shift) is readily detectable. The system was operated at 20× magnification, yielding a spatial resolution of ~10 μm at the target.

Preliminary Experiments

We performed a series of preliminary experiments to demonstrate the utility of this diagnostic. In our first experiment, a 250-μm-thick silicon flat coated with 100 nm of Al on the drive side was irradiated with one Nova laser beam at 2ω (532 nm). The drive-laser spatial profile was spatially smoothed by a kinoform phase plate[19] and was ellipsoidal with major and minor axes of 900 and 600 μm, respectively. The drive laser had an 8-ns, temporally square profile with a rise time of 100 ps, producing an intensity of $\sim 8 \times 10^{13}$ W/cm^2 at the target. Figure 3(a) shows the data from this experiment. Motion is detected about 1.3 ns before the shock breaks through the rear surface of the Al fringe, which corresponds to an expansion velocity of $\sim 3 \times 10^4$ cm/s. The predicted shock breakout time for this irradiance according to calculations using the LASNEX code was ~9.9 ns. Observations indicate that this predicted breakout time is correct to within the error in the experimental timing, which is ±500 ps.

In our second experiment, an Al target consisting of side-by-side steps 50 and 100-μm thick, respectively, with a 15-μm-thick polystyrene ablator coated onto the drive side, was irradiated at an intensity of $\sim 7.7 \times 10^{13}$ W/cm^2. As seen in Figure 3(b), fringe motion is detected prior to shock breakout on the 50-μm step of Al, but no motion is detected at the rear surface of the 100-μm step. The observed shock breakout times are about 2.2 ns for the 50-μm step and 4.3 ns for the 100-μm step, which are in good agreement with our predictions. A small amount of fringe motion on the 100-μm step immediately adjacent to the step's edge is attributed to edge effects brought on by the earlier breakout of the 50-μm step, not preheating of the sample through the bulk Al. Here, the expansion velocity is about 3.5×10^4 cm/s. The shock velocity in the Al is 26 μm/ns based on the relative breakout times for the two steps compared to a predicted shock velocity of 25 μm/ns with LASNEX simulations.

Because the expansion velocity is two orders of magnitude below the shock velocity, we can indeed attribute the expansion to preheat. The source of the preheat for the Al step target is likely x rays with energies just under the Al k-edge at 1.56 keV. Because the temperature in the laser deposition region is 1 to 2 keV, there is a significant x-ray flux at this frequency.

Characterization of the Cryogenic Cell Targets

Figure 1 shows the design of the cryogenic cell targets. The Al pusher was machined in a "tophat" geometry so that the rear surface of the pusher would always protrude exactly the same distance into the

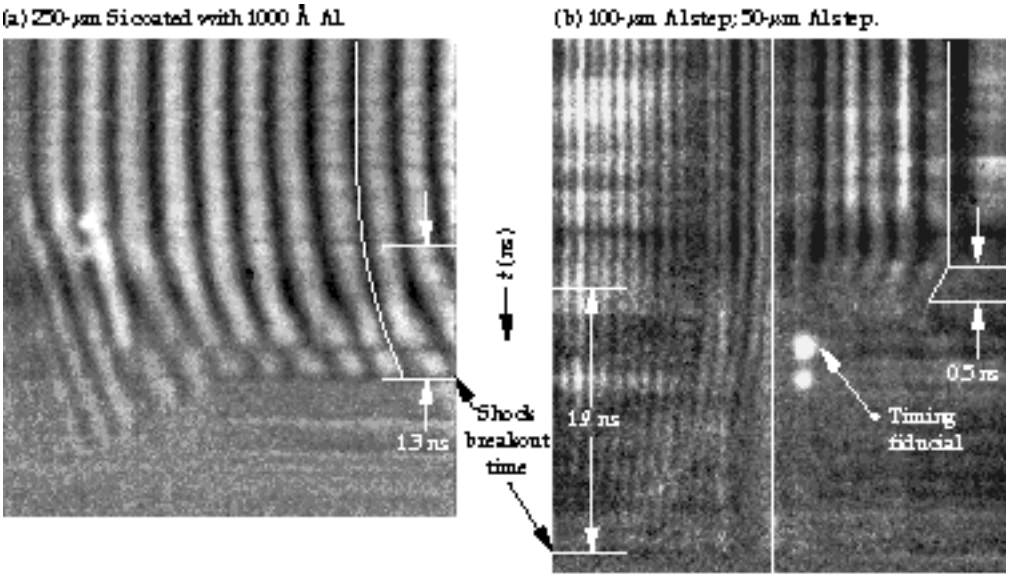

FIGURE 3. Streak camera records of the shock passing through (a) a 250-μm-thick silicon flat coated with a 1000-Å Al layer, where motion of the rear surface in advance of the shock wave is clearly observed, indicating that this surface is preheated; (b) a target with a 100-μm Al step placed next to a 50-μm Al step, where minimal or no fringe motion is detected on the 100-μm Al step side of the image, while preheat-induced thermal expansion is clearly observed on the 50-μm Al step side.
(08-00-0197-0008pb01)

cryogenically cooled D_2 reservoir regardless of the pusher's thickness. Thus, the side of the pusher where the Nova drive beam was incident was more reentrant for thinner pusher geometries. The Al thickness was varied between 100, 180, and 250 μm, and the Al pushers were 1 mm in diameter. The pusher was coated with 20 μm of polystyrene as an ablator, which was subsequently overcoated with 100 nm of Al to prevent direct laser shine through the polysterene at the onset of the drive laser pulse. The probe laser beam was reflected off the rear surface of the Al pusher after passing through a sapphire window and a 0.5-mm-long reservoir filled with liquid D_2, and the entire cell assembly was cooled to a temperature of 19.4 to 19.8 K.

Figure 4(a) shows the interferogram generated when a 100-μm-thick pusher with a 20-μm-thick polystyrene ablator was driven at about 1.5×10^{14} W/cm^2. Motion of the D_2–Al pusher interface is clearly observed beginning ~2 ns prior to shock breakout. A simple thermal expansion model estimates the temperature at this surface to be ~1000 K. The shock breakout was predicted to occur ~4.3 ns after initiation of the drive laser pulse for these conditions, so some preheating of the Al occurs early in the 8-ns-duration, laser-driven pulse. Because any high-energy x rays that penetrate the pusher are unlikely to be absorbed in the D_2, any heating of the D_2 is a consequence of thermal conduction from the Al. Any such D_2 preheat is negligible for the strong shocks considered in these experiments. The shock is planar over the central 400 μm of the target, with rarefaction waves moving inward from the edges causing the observed curvature.

When the intensity on this target was turned down to about 8.5×10^{13} W/cm^2, no evidence of preheating was observed, as shown in Figure 4(b). Again, the shock is planar over ~400 μm; however, a second region of shock curvature is observed. This structure is attributed to the reentrant nature of the Al pusher design. Al plasma generated by the drive laser beam moves into the path of the beam during its 8-ns duration, effectively reducing the intensity of the drive pulse on the outer perimeter of the Al pusher and slowing down the shock considerably at the target's edges.

Interferograms of the thicker pushers (180 and 250 μm) showed no fringe shifts, indicating that there was no motion at the rear surface. For a detection limit of 0.2 fringe, which corresponds to movement of 30 nm at the pusher surface, the maximum surface temperature of the pusher for these targets prior to shock breakout is estimated to be <400 K.

Future Directions

To produce stronger shocks and investigate both direct- and indirect-drive schemes for generating shock waves, we are planning future investigations of a variety of materials for the Nova ten-beam facility. This will allow multiple drive laser beams to be overlapped in a direct-drive geometry and will allow the use of hohlraum drivers to produce stronger shocks and higher pressures. Preheating is a significant concern, particularly in the case of indirectly driven targets where large quantities of Au M-band x rays ($E > 2$ keV) are generated. We are currently integrating this interferometric characterization diagnostic onto the ten-beam facility. To avert potential problems with background radiation from the Nova drive

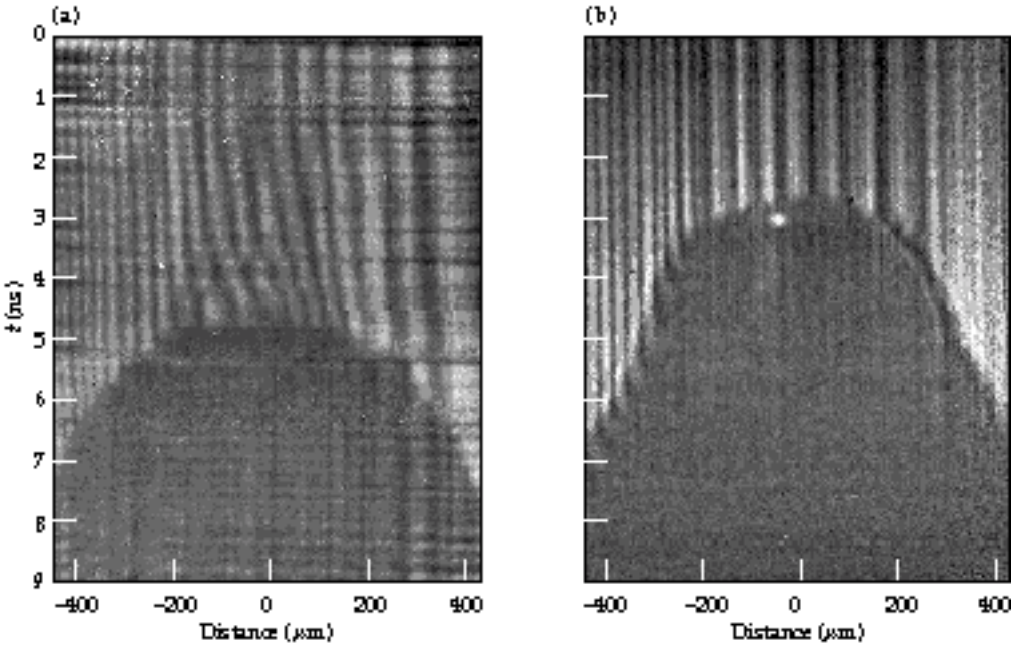

FIGURE 4. (a) Intensity of ~1.5 × 10^{14} W/cm^2 incident on a 100-μm-thick Al pusher coated with 20 μm of polystyrene and 100 nm of Al. Expansion of the rear surface due to preheating is clearly observed. (b) Intensity of ~8.5 × 10^{13} W/cm^2 incident on the same target described in (a). Here, no motion of the rear surface is observed prior to shock breakout. The shaping of the breakout may be caused by Al plasma generated on the drive laser side of the target moving into the path of the drive beam. (08-00-0197-0009pb01)

beams, the laser system used will be an injection-seeded, Ti:Sapphire regenerative amplifier operating at a wavelength (λ = 403 nm) anharmonic relative to standard Nova frequencies. This wavelength is produced by frequency-doubling the 807-nm fundamental of the Ti:Sapphire. We have designed an f/3 imaging system to relay the probe laser beam to the target and image the evolving target system. The first phase of activation incorporates only displacement interferometry, but we are planning an upgrade to a VISAR system.

Conclusions

Interferometric techniques provide an accurate method for determining both the spatial and temporal characteristics of laser-driven shock waves. We used a Michelson interferometer in situ on the two-beam facility at Nova to evaluate both the level of preheating present under a variety of conditions and the spatial uniformity and planarity of the incident shock wave. Using the interferometer, we were able to determine that there were insignificant levels of preheat due to the laser drive and that the driver was shown to generate a shock that remained planar over approximately the central one-third of the target throughout the experiment. With further modeling efforts, the motion of the target's rear surface in advance of the shock breakout could be directly correlated to the temperature of this surface, thus providing a very accurate preheat diagnostic for laser-driven shock experiments. This technique is currently being integrated into the suite of diagnostics available in the ten-beam facility at Nova. The first demonstrations of interferometric characterization of shock-driven targets were conducted in December 1996.

Acknowledgments

The authors gratefully acknowledge the expert technical support of J. Cardinal, D. Cocherell, T. Weiland, and the entire technical staff at the Nova laser facility. We also thank S. G. Glendinning for valuable assistance with image-processing techniques.

Notes and References

1. C. E. Ragan III, M. G. Silbert, and B. C. Diven, *J. Appl. Phys.* **48**, 2860–2870 (1977).
2. C. E. Ragan III, *Phys. Rev. A* **29**, 1391–1402 (1984).
3. A. Vladimirov, N. P. Voloshin, V. N. Nogin, A. V. Petrovtsev, and V. A. Simonenko, *JETP Lett.* **39**, 82–85 (1984).
4. E. N. Avrorin, B. K. Voldolaga, N. P. Voloshin, V. F. Kuropatenko, G. V. Kovalenko, et al., *JETP Lett.* **43**, 308–311 (1986).
5. A. C. Mitchell, W. J. Nellis, J. A. Moriarty, R. A. Heinle, N. C. Holmes, et al., *J. Appl. Phys.* **69**, 2981–2986 (1991).
6. L. R. Veeser and S. C. Solem, *Phys. Rev. Lett.* **40**, 1391–1394 (1978).
7. R. J. Trainor, J. W. Shaner, J. M. Auerbach, and N. C. Holmes, *Phys. Rev. Lett.* **42**, 1154–1157 (1979).
8. C. G. M. van Kessel and R. Sigel, *Phys. Rev. Lett.* **33**, 1020–1023 (1974).
9. S. P. Obenschain, R. R. Whitlock, E. A. McLean, B. H. Ripin, R. H. Price, et al., *Phys. Rev. Lett.* **50**, 44–48 (1983).
10. F. Cottet, J. P. Romain, R. Fabbro, and B. Faral, *Phys. Rev. Lett.* **52**, 1884–1886 (1984).
11. K. A. Tanaka, R. Kodama, K. Nishihara, M. Kado, A. Nishiguchi, et al., in *Shock Waves*, K. Takayama, Ed. (Springer-Verlag, Berlin, 1992), p. 863.
12. T. Löwer, R. Sigel, K. Eidmann, I. B. Földes, S. Hüller, et al., *Phys. Rev. Lett.* **72**, 3186–3189 (1994).
13. A. M. Evans, N. J. Freeman, D. Graham, C. J. Horsfield, S. D. Rothman, et al., *Lasers Part. Beams* **14**, 113–123 (1996).
14. R. Cauble, D. W. Phillion, T. J. Hoover, N. C. Holmes, J. D. Kilkenny, and R. W. Lee, *Phys. Rev. Lett.* **70**, 2102–2105 (1993).
15. R. Cauble, L. B. Da Silva, S. G. Glendinning, S. M. Lane, T. S. Perry, and D. W. Phillion, *1993 ICF Annual Report*, **6**(4)131–136, Lawrence Livermore National Laboratory, Livermore, CA, UCRL-LR-105820-93 (1993).
16. L. B. Da Silva, P. Celliers, G. W. Collins, K. S. Budil, N. C. Holmes, et al., *Phys. Rev. Lett.* **78**, 483 (1997).
17. L. M. Barker and R. E. Hollenbach, *Rev. Sci. Instrum.* **36**, 1617–1620 (1965).
18. L. M. Barker and R. E. Hollenbach, *J. Appl. Phys.* **43**, 4669–4675 (1972).
19. S. Dixit, Lawrence Livermore National Laboratory, Livermore, CA, private communication (1996).